Journal of Sound and Vibration (1999) **224**(5), 785–808
Article No. jsvi.1998.2182, available online at http://www.idealibrary.com on IDEAL®

INTERACTION OF THE ACOUSTIC PROPERTIES OF A COMBUSTION CHAMBER WITH THOSE OF PREMIXTURE SUPPLY

C. J. LAWN

Department of Engineering, Queen Mary and Westfield College, University of London, London E1 4NS, England

(*Received* 30 *July* 1998)

If the response of a flame to acoustic waves is not known, it must be deduced from measurements in a system for which the acoustic impedances can be inferred. Measurements have been made on a simple combustion system in which gaseous propane is mixed with air in a cylindrical chamber of variable length before flowing up a burner tube. At the end of the tube, the premixture flows around a centre-body, behind which a flame is stabilized. When placed in cylindrical combustion chambers of two different lengths, the flame generates self-excited acoustic oscillations. These have been measured with pressure transducers at three different points and with a system for collecting the UV radiation from the whole flame at a wavelength of chemiluminescent emission. The data demonstrate that the acoustic transmission through the premixture supply system and through the combustion chamber can be described by standard one-dimensional acoustic theory, provided an appropriate choice of mean speed of sound in the combustion chamber is made. This then allows the jump in the volumetric acoustic fluxes across the flame to be calculated, and it is shown, by examination of the magnitude and phase of the transfer function, that this jump is proportional to the UV emission over a range of frequencies up to 800 Hz (a frequency corresponding to wavelengths of the order of the combustion chamber length). This relationship is in accordance with thermo-acoustic theory for a "thin" flame, if the UV emission can be taken as proportional to the instantaneous rate of heat release. The observations therefore validate both the experimental technique and the applicability of the theoretical assumptions, and lay the foundation for a more detailed study of the structural response of the flame.

1. INTRODUCTION

Following the pioneering work of Lord Rayleigh [1], the principles of the self-excitation of acoustic modes in combustion systems have been well established in terms of the acoustic properties of the ducts upstream and downstream of the flame, and of the acoustic transfer function of the flame region [2–4]. Unfortunately, the transfer function of the flame is usually unknown *a priori* and must be determined empirically. Since direct measurement of the transfer function is not usually

0022-460X/99/300785 + 24 $30.00/0

possible either, due to the high temperatures in the flame zone, it must be deduced for a particular firing condition from the relationship between the acoustic impedances upstream and downstream, and then some flame model must be used to extrapolate the overall system behaviour to other firing conditions.

From this perspective, the "passive" acoustic conditions place a thermo-acoustic constraint on the flame transfer function across the total frequency spectrum, and the combustion response determines the eigenfrequencies at which the total system will respond with high amplitude. The alternative approach is therefore to propose a model for the flame and then to solve the complete set of equations for the eigenfrequencies. This has been achieved for a multi-port burner [3], for simple tubes [3, 4] and for a dump combustor [5], but the procedure has the disadvantage that the individual components of error are not readily identified.

It is clearly essential to obtain a satisfactory description of the acoustic properties of both the air and fuel supply systems, and of the combustion chamber and flue-gas system. It is the purpose of this paper to show for a flame of propane and air with a simple premixture supply system and cylindrical combustion chamber that one-dimensional acoustic theory is adequate to describe the acoustic conditions on either side of the flame. Measurements of the chemiluminescent UV emission, which is indicative of the heat release rate, are then found to have the expected theoretical relationship to the jump in acoustic volumetric flux across the flame.

These checks are essential preliminaries to a study of the variation in the heat release rate up the height of the flame, and its fluctuation in time, since this information must form the basis of any model. They demonstrate that the technique can be used in analysing the thermo-acoustic behaviour of more complex flames and premixture supply systems. The particular relevance of premixed gaseous combustion is to the land-based gas turbine, in which a lean premixture is burnt in order to suppress NO_x emissions.

2. APPARATUS

Air from the laboratory supply system was fed through a rotameter to a cylindrical plenum where it was mixed with propane jetting out of tiny holes in a central supply pipe, after having also been metered by rotameter (Figure 1). The volume of the plenum could be adjusted by moving the plunger base. Two configurations were deployed in the present study: ones having a plenum depth of 134 mm and of 63 mm. The former arrangement was coupled with a real acoustic impedance at the base of the burner tube in the form of a disk with eight symmetrically arranged holes covered by fine mesh gauze. The two plenum geometries will be referred to as having "high" and "low" impedance, respectively. An Electret condenser microphone recorded the pressure fluctuations at the top of the plenum.

From the top of the plenum, the mixture flowed up the burner tube and around a body which was streamlined on the upstream side and had a downstream-facing disk which was flush with the end of the tube. A smooth transition to a higher

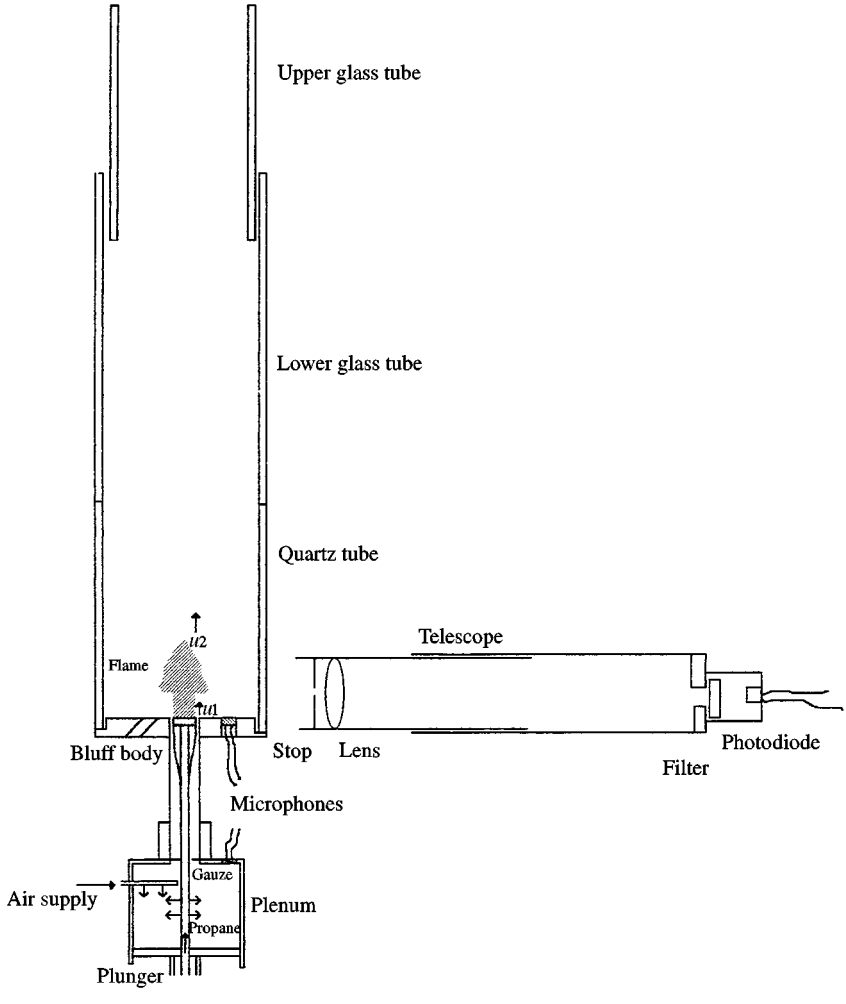

Figure 1. The apparatus.

radius ratio annular jet was thereby created, together with a substantial recirculation zone in the wake. Over a wide range of conditions, the flame was firmly anchored through this recirculation of hot products, and exhibited a pale blue region with the shape shown in Figure 1, the annular jet of fresh premixture igniting in tongues some 20–30 mm above the burner exit. The base of the combustion chamber was also flush with the end of the burner tube and it contained another condenser microphone to record the pressure fluctuations in the flame zone.

The combustion chamber walls comprised a section of quartz, butted against a glass tube of the same diameter, 100 mm, to make a continuous length of 625 mm. A second glass tube slid inside the first to make an adjustable length and an almost constant diameter, about six times that of the inner diameter of the burner tube. Two lengths of chamber were tested in the current experiments: 625 and 888 mm. The top of the combustion chamber was open to the laboratory and had no flange.

In some experiments, a third condenser microphone was deployed for short periods at the tube wall in the exit plane, until it failed due to overheating.

The transfer function between the amplified signals from the pressure transducers in pairs was evaluated on a Hewlett–Packard spectrum analyzer over the frequency range from 0 to 800 Hz. The upper frequency limit was chosen because it embraced most of the energy-containing spectrum. A bandwidth of 4 Hz was chosen and 60 averages were taken in order to effect the best compromise between accuracy and speed of acquisition.

Alongside the pressure transducer, two channels of UV signal were also stored. These signals were produced by amplifiers attached to photodiodes on the end of telescopic viewing systems, one of which is shown in Figure 1. Each telescope had a 51 mm quartz lens to collect the radiation, which fell on the photodiode after transmission through a narrow-bandpass filter. This filter passed UV radiation in the 307 ± 5 nm bandwidth, which is due to a chemiluminescent transition, and can be taken to be instantaneously related to the heat release [6]. One telescope was fixed in position so that the photodiode responded to radiation from virtually the whole of the flame, from 0 to 45 mm above the burner tube exit. The other was arranged at right angles to the first and had a narrow horizontal slit in front of the lens. It thus responded only to radiation from a slice of the flame. The local measurements from this device will be reported separately. Here we are concerned only with the total flame emission, representative of the instantaneous heat release from the whole flame.

3. SCOPE OF THE MEASUREMENTS

With two values of plenum impedance, and two lengths of combustion chamber, it was intended to take measurements for four different geometric conditions. In the event, with a fuel flow rate of 1·0 l/min, it proved impossible to stabilize a flame at any equivalence ratio with the low impedance plenum and the long combustion chamber. For the other three geometries, measurements are reported for two air flow rates, ranging from rich to lean. There are thus only six complete sets of measurements in which the heat release was measured, but in preliminary runs, the pressure transfer function from plenum to flame, and from flame to combustion chamber outlet, were each recorded at the two air flow rates. These were generally 20 and 30 l/min, corresponding to equivalence ratios of 1·2 and 0·8, respectively, although in one instance, the stoichiometric condition with 24 l/min was selected. The highest flow rate gave rise to a velocity of 5 m/s in the burner exit annulus, a jet Reynolds number of 1500.

Measurements of the mean flow pressure distribution confirmed that the pressure in the propane rotameter at the higher flow rate was only 4% above the atmospheric pressure. However, the loss through the supply system, due principally to the sparge holes in the plenum, was nevertheless sufficient to ensure that the acoustic pressure fluctuations in the plenum (about 100 Pa) gave rise to only small fluctuations in the fuel supply (about 1%). These would have been damped out by mixing in the plenum, Similarly, the mean excess pressure in the air supply was also

about 4%, and so the bottom of the plenum can be assumed to be an acoustic termination.

The data indicated mean flow pressure loss coefficients referred to the full area of the burner tube of $K = 39$–41 (depending on flow rate) for the high impedance plenum and $K = 10$ for the low impedance one. The pressure loss coefficient is required when assessing the real acoustic impedance of the system, as seen from the following theory.

4. ACOUSTIC THEORY

Acoustic transmission in a uniform duct in which there are frictional losses may be described (to first order) by the perturbed form of the 1-D continuity and momentum equations for a mean flow velocity $\bar{U}$ and density $\bar{\rho}$, and acoustic fluctuations, u, ρ', and p (a list of notations is given in Appendix B):

$$\frac{\partial \rho'}{\partial t} + \bar{\rho}\,\frac{\partial u}{\partial x} + \bar{U}\,\frac{\partial \rho'}{\partial x} = 0, \tag{1}$$

$$\bar{\rho}\,\frac{\partial u}{\partial t} + \bar{U}\,\frac{\partial \rho'}{\partial t} + \frac{\partial p}{\partial x} + \left(\frac{\partial}{\partial x} + \frac{K}{2l}\right)(2\,\bar{\rho}\,\bar{U}u + \rho'\,\bar{U}^2) = 0, \tag{2}$$

where K is the overall loss coefficient, distributed uniformly over a length l. The perturbed form of the energy equation for a perfect gas in the presence of a chemical heat release fluctuation q per unit volume, upon ignoring the small entropy production due to the frictional losses and assuming the fluctuations are rapid enough to be adiabatic, is [7]

$$\frac{\mathrm{d}\rho'}{\mathrm{d}t} = \frac{1}{c^2}\left(\frac{\mathrm{d}p}{\mathrm{d}t} - (\gamma - 1)\,q\right), \tag{3}$$

where $c^2 \equiv (\partial \bar{p}/\partial \bar{\rho})_s$ is the speed of sound and γ is the ratio of specific heat capacities.

In the absence of heat release, the energy equation yields

$$p = c^2\,\rho' = \gamma\,R\bar{T}\,\rho', \tag{4}$$

and for a lossless system, $K = 0$, the characteristic equation for a solution $u \propto \mathrm{e}^{\mathrm{i}(\omega t \pm k^* x)}$ is

$$-\omega^2 + c^2(1 - M^2)\,k^{*2} \mp 2\,Mc\omega k^* = 0, \tag{5}$$

so that

$$k^* = k/(1 \pm M) \tag{6}$$

for waves propagating with and against the flow, where k satisfies the normal wave equation and is given by $k = \omega/c$, and $M \equiv \bar{U}/c$ is the Mach number of the mean flow.

However, if $M \ll 1$, these convection velocities can be ignored and the solutions to the modified spatial wave equation

$$\partial^2 u/\partial x^2 + k^{*2} u = 0 \tag{7}$$

for $K \neq 0$ are

$$k^* = k\sqrt{1 - \mathrm{i}KM/kl}, \tag{8}$$

where there are two (complex) roots. The roots can be written as

$$k^* = k' + \mathrm{i}k'' = \pm k\sqrt{\tfrac{1}{2}\sqrt{1+\alpha^2} + \tfrac{1}{2}} \mp \mathrm{i}k\sqrt{\tfrac{1}{2}\sqrt{1+\alpha^2} - \tfrac{1}{2}}, \tag{9}$$

where $\alpha = KM/kl$.

Now for a duct with inlet conditions (p_i, u_i) and outlet conditions (p_0, u_0), the solutions to the wave equation can be written as

$$\bar{\rho}\, c u_0 = -\mathrm{i}\, p_i\, (k/k^*) \sin k^* l + \bar{\rho}\, c\, u_i \cos k^* l \tag{10}$$

and

$$p_0 = p_i \cos k^* l - \mathrm{i}\, \bar{\rho}\, c\, u_i\, (k^*/k) \sin k^* l, \tag{11}$$

so the transfer function is

$$p_0/p_i = \cos k^* l - \mathrm{i}\, (k^*/Z_i\, k) \sin k^* l, \tag{12}$$

where Z_i is the inlet impedance. Moreover, the outlet impedance can be expressed in terms of Z_i by dividing equation (11) by equation (10). Thus, transmission through a series of ducts with different characteristics can be calculated by expanding the complex equations (9–11) into real and imaginary parts (involving combinations of trigonometric and hyperbolic functions) and calculating sequentially on a spreadsheet, starting with a known acoustic termination such as a closed end ($Z_i \to \infty$) or an open unflanged pipe of diameter d [8], for which

$$Z_i = 0{\cdot}062\, k^2 d^2 + \mathrm{i}\, 0{\cdot}306\, kd, \tag{13}$$

and adjusting the acoustic velocities to take account of the flow cross-section.

To calculate the impedance of the plenum and burner combination, as seen from the flame zone, for example, the bottom of the plenum is taken to be a closed end and transmission (lossless) to the top is calculated. The loss in the burner tube is taken to be distributed, even though it is clearly concentrated at the bottom when the gauze is in place, and the impedance at the inlet to the tube is calculated from the ratio of the flow areas in the plenum and tube, assuming the pressures to be continuous. The impedance at the top of the burner tube can then be related to the relevant exit flow area. The mean speed of sound for the premixture supply system is taken to be that of air at ambient temperature.

For the combustion chamber, a single calculation down to the flame zone from a termination given by equation (13) with an estimated speed of sound at the exit of 400 m/s, was made. Losses in the chamber were neglected. The appropriate mean speeds of sound were taken as 600 m/s for the 625 mm combustion chamber, and 550 m/s for the 888 mm one. These values were chosen with reference to the acoustic data.

For the flame zone, with M still $\ll 1$, substitution of equation (1) in equation (3) gives

$$\frac{\partial u}{\partial x} = -\frac{1}{\bar{\rho} c^2}\left(\frac{\partial p}{\partial t} - (\gamma - 1)\, q\right). \tag{14}$$

However, the flame zone is thin compared with the wavelengths considered here, since these are never much less than the length of the chamber, and in this case the pressure term can be disregarded in the low Mach number limit. Integrating over the volume of the flame zone, shows that

$$u_2\, A_2 - u_1\, A_1 = \frac{(\gamma - 1)}{\bar{\rho}\, c^2} \int q \, \mathrm{d}A \, \mathrm{d}x = \frac{(\gamma - 1)}{\bar{P}\, \gamma}\, h, \tag{15}$$

where the areas are those over which the acoustic velocities are distributed. This demonstrates a "velocity jump" (actually a "volumetric flux jump") proportional to the total heat release fluctuation h. By the same approximation, integration of equation (2) shows that p is continuous across the flame. Thus, a single acoustic pressure p_f is adequate to describe conditions at exit from the burner and at the bottom of the combustion chamber, even when there is a flame between them.

5. RESULTS

5.1. RESULTS FOR THE PREMIXTURE SUPPLY SYSTEM

The spectra of the pressure fluctuations in the flame zone, p_f, and in the plenum, p_w, are shown in Figure 2 for the high impedance plenum. Clearly, while the flame is experiencing significant fluctuations in the frequency bands from 50 to 350 Hz and from 600 to 750 Hz, with intensity varying according to flow rate, the plenum is mostly responding at 75 Hz, which is in fact the Helmholtz resonance frequency for this configuration of plenum and burner.

Nevertheless, the data in Figure 3 demonstrate that there is significant coherence, $Co(wf) = [\overline{p_f\, p_w}/\tilde{p}_f\, \tilde{p}_w]$, over most of the spectrum, with the exception of the range 400–500 Hz.

The variation of the magnitude of the transfer function $|\, Tr\,(f/w)| = |\,\overline{p_f\, p_w}/\overline{p_w^2}\,|$, is shown in Figure 4. Where the coherence is very low, $Co < 0{\cdot}2$, the transfer function has been recorded as zero and disregarded, because jet noise in the plenum is contaminating the signal. Without contamination, this function should have the value of the transfer function p_f/p_w computed by the methods of the last section, although it must be noted that there is a substantial uncertainty in the absolute magnitude, due to a difference in the calibration of the two transducers. (This varied according to the temperature at which they were run.) The small difference between the predictions for the two flow rates is due to the difference in real impedance. It is seen that the measurements follow broadly the theoretical variation, although the very high peak values calculated for 650 Hz are not realized in practice, the measured maximum being about 250, probably because of the additional plenum noise which does not propagate as a plane wave up the burner tube.

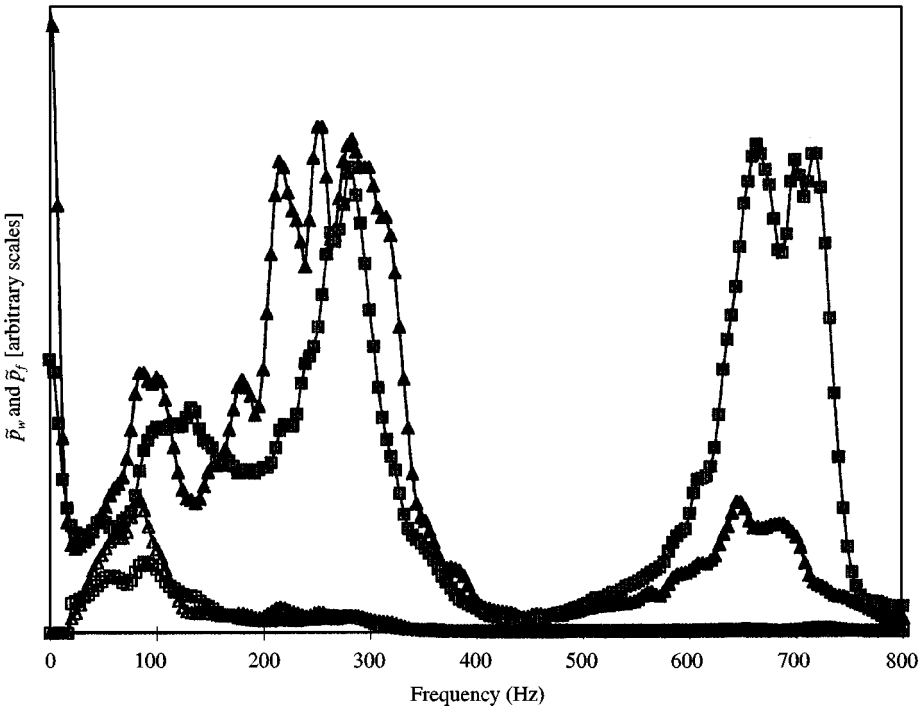

Figure 2. Plenum and flame zone pressures for the high impedance plenum (combustion chamber length = 625 mm). —△—, $\tilde{p}_w$; $V_a = 20$ l/min; —□—, $\tilde{p}_w$; $V_a = 30$ l/min; —▲—, $\tilde{p}_f$; $V_a = 20$ l/min; —■—, $\tilde{p}_f$, $V_a = 30$ l/min.

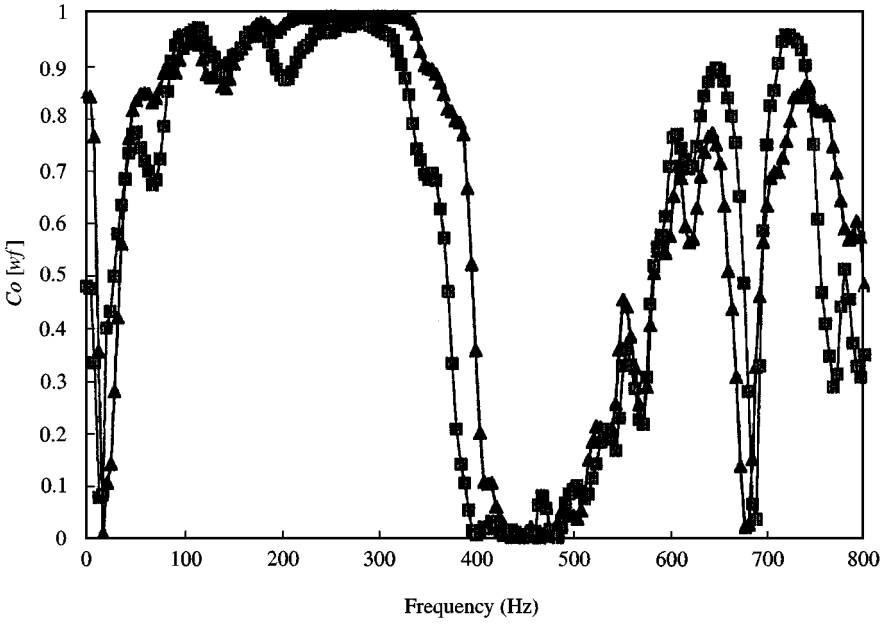

Figure 3. Coherence between plenum and flame zone pressures for the high impedance plenum (combustion chamber length = 625 mm). —▲—, $V_a = 20$ l/min; —■—, $V_a = 30$ l/min.

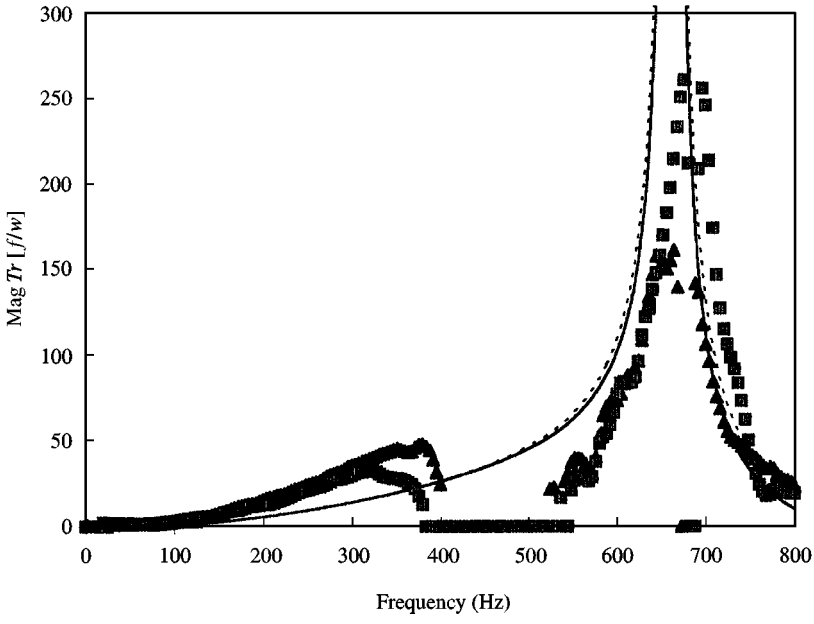

Figure 4. Transfer function between plenum and flame zone pressure with $Co > 0{\cdot}2$ for the high impedance plenum (combustion chamber length = 625 mm). ▲, $V_a = 20$ l/min; ■, $V_a = 30$ l/min; ———, theory, $V_a = 20$ l/min; – – – –, theory, $V_a = 30$ l/min.

The phase between the two pressures is, however, very closely predicted up to 700 Hz, where a divergence occurs (Figure 5). The variation in the damping with flow rate is reflected in the measurements at the Helmholtz frequency. Once again, the measurements have been disregarded where the coherence is low. Although there should be no bias in the data due to noise, the random contributions do degrade the accuracy with which it is measured. The consistency of the phase variation appears to show that $Co > 0{\cdot}2$ is an adequate criterion.

Similar results were obtained for the low impedance plenum, the lower flow rate in this case being 24 l/min. However, the plenum pressure was much more sharply peaked at the Helmholtz resonance of the plenum/burner combination (110 Hz) and exceeded the flame zone pressure. The magnitude of the transfer function, both according to theory and experiment, peaked at a value of only 12–13 at 600 Hz. The phase variation again showed significant discrepancies between theory and experiment above 750 Hz, but it was closely in accord elsewhere, upon taking account of the 360° ambiguity in the measurements.

5.2. RESULTS FOR THE COMBUSTION CHAMBER

The spectra in Figure 6 for p_f are a repeat of those in Figure 2 for the 625 mm combustion chamber and hence illustrate the degree of variability encountered in the precise levels of excitation. This appeared to be due to variations in the degree of heating of the apparatus. Nevertheless, it is seen that the major trends with frequency

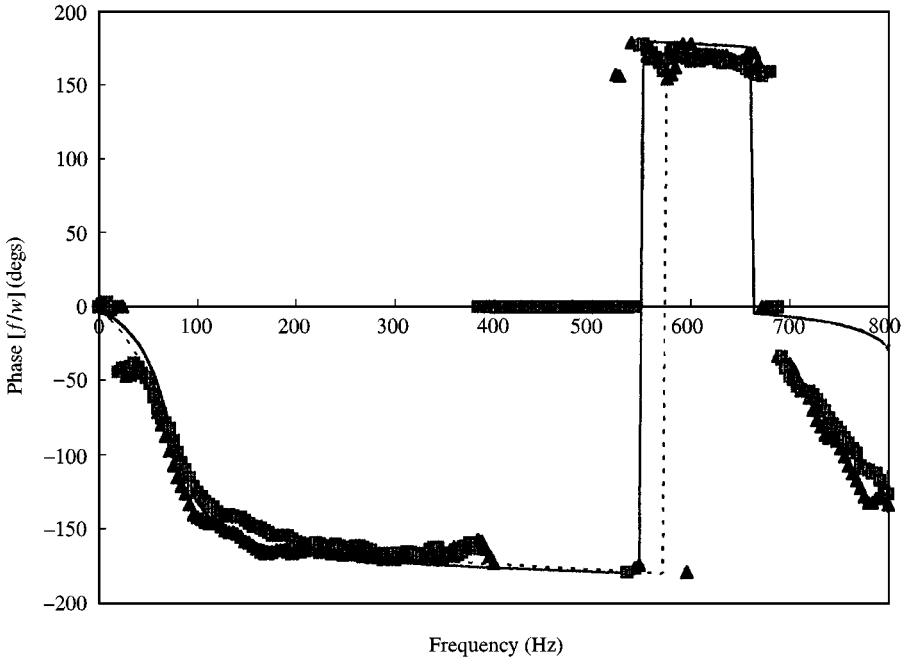

Figure 5. Phase of the plenum pressure relative to the flame zone with $Co > 0{\cdot}2$ for the high impedance plenum (combustion chamber length = 625 mm). ▲, $V_a = 20$ l/min; ■, $V_a = 30$ l/min; ———, theory, $V_a = 20$ l/min; – – – –, theory, $V_a = 30$ l/min.

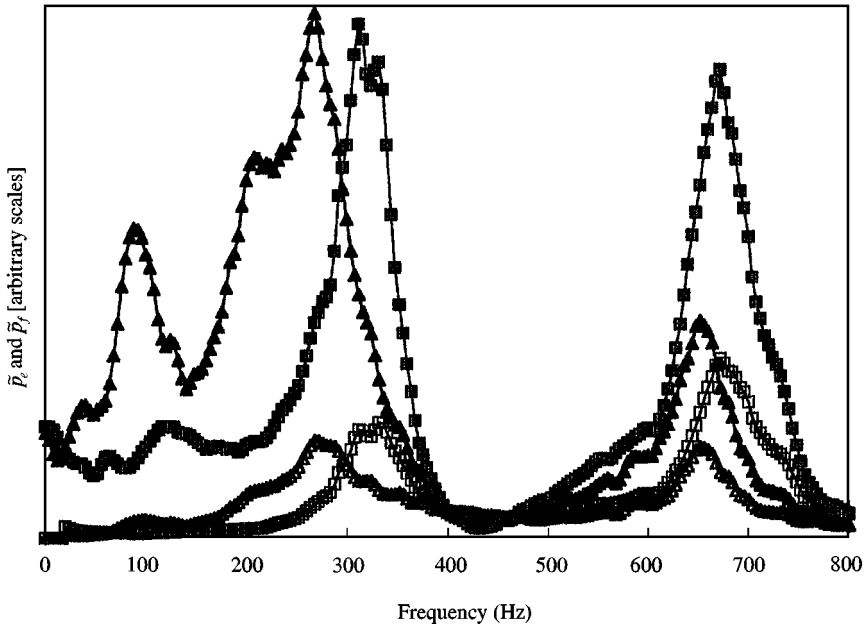

Figure 6. Combustion chamber exit and flame zone pressures for the high impedance plenum. (combustion chamber length = 625 mm). —△—, $\tilde{p}_e$; $V_a = 20$ l/min; —□—, $\tilde{p}_e$; $V_a = 30$ l/min; —▲—, $\tilde{p}_f$; $V_a = 20$ l/min; —■—, $\tilde{p}_f$, $V_a = 30$ l/min.

and air flow rate (or equivalence ratio) are reproduced. Fluctuations in pressure at the combustion chamber exit, p_e, mirror the trends in p_f, but at a lower level.

The coherence between the two combustion chamber pressures (at exit and in the flame zone) is high everywhere in the spectrum, except in the ranges 0–100 and 400–500 Hz (Figure 7).

The trends in the magnitude of the transfer function are accurately predicted down to 100 Hz, when adequate coherence is lost (Figure 8). It emerges that the loss of coherence in the range 400–500 Hz is associated with a true minimum in the transfer function at 450 Hz, which corresponds to a half-wave mode in the combustion chamber.

Phase variations are less well predicted (Figure 9), although the qualitative trends are correct. Below 200 Hz, there is a 30–50° discrepancy, even where the coherence is high.

The results for the longer combustion chamber, 888 mm, were qualitatively similar to those for 625 mm, although sharper peaks in excitation appeared, at 150, 450 and 750 Hz, corresponding to the 1/4, 3/4 and 5/4 wavelength modes, and coherence was lost at 300 and 600 Hz, the half- and full-wavelength modes. The same type of discrepancy was seen in the phase predictions as for the shorter chamber, but to a lesser extent.

5.3. RESULTS FOR THE HEAT RELEASE

Another set of data for the flame zone pressure spectrum in the 625 mm combustion chamber with the high impedance plenum was taken in conjunction

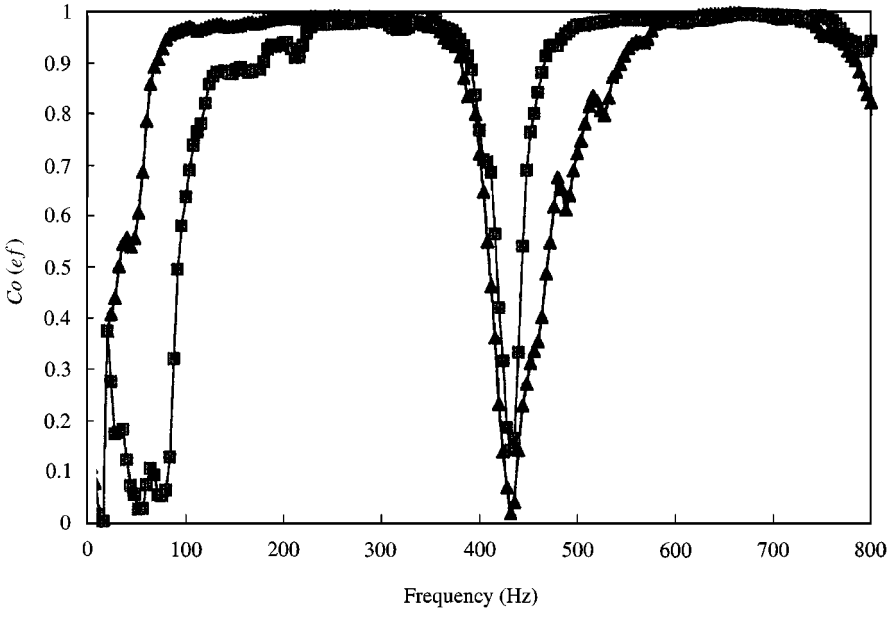

Figure 7. Coherence between the combustion chamber exit and flame zone pressures for the high impedance plenum (combustion chamber length = 625 mm). —▲—, $V_a = 20$ l/min; —■—, $V_a = 30$ l/min.

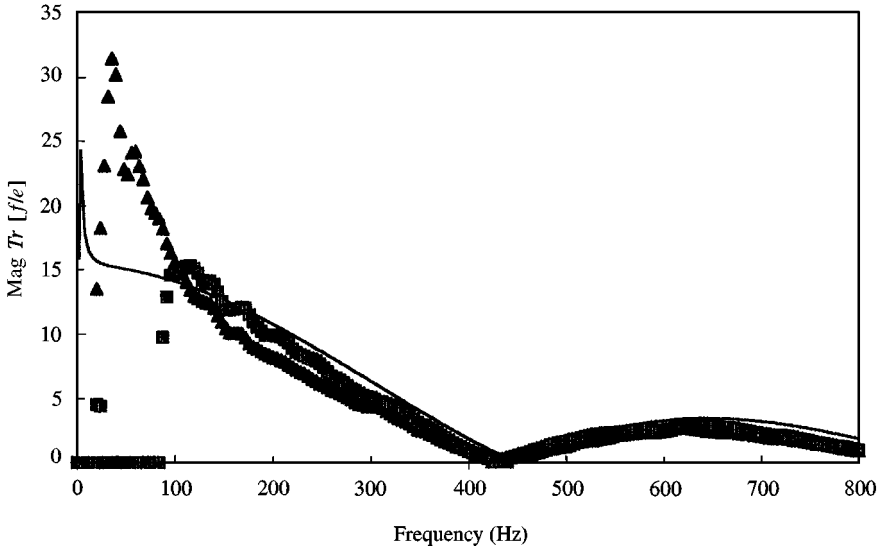

Figure 8. Transfer function between combustion chamber exit and flame zone pressures with $Co > 0{\cdot}2$ for the high impedance plenum (combustion chamber length = 625 mm). ———, theory; ▲, $V_a = 20$ l/min; ■, $V_a = 30$ l/min.

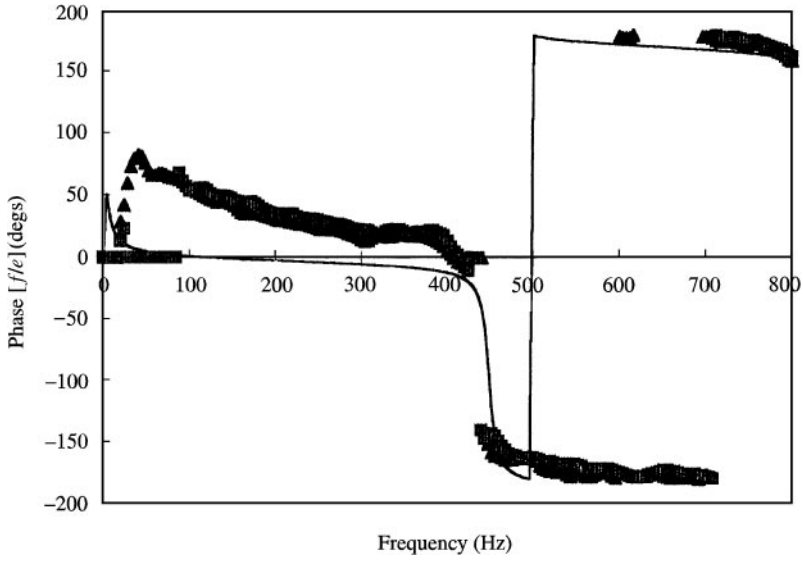

Figure 9. As Figure 8 but for the phase of the exit pressure relative to the flame zone pressure.

with the UV emission data from the whole flame, designated signal b and assumed proportional to the heat release h for a given equivalence ratio. Similar, but not identical, spectra of p_f and b are observed for each of the two equivalence ratios, and there was indeed strong coherence between these two signals in many parts of the spectrum.

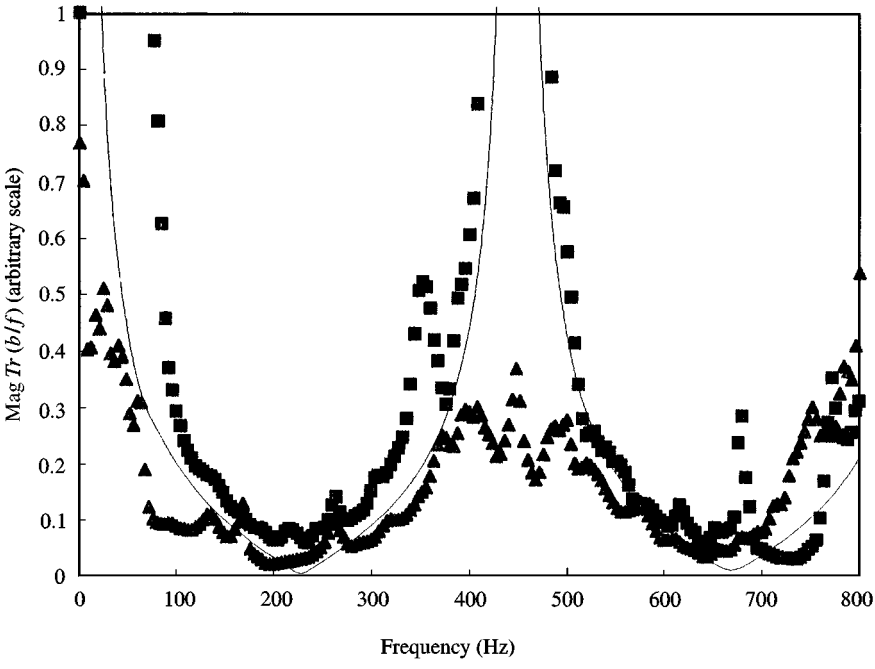

Figure 10. Magnitude of the transfer function between the total UV emission or the predicted acoustic velocity jump and the flame zone pressure for the high impedance plenum (combustion chamber length = 625 mm). ———, theory for $A_2u_2 - A_1u_1$, $V_a = 20$ and 30 l/min. Total UV emission: ▲, $V_a = 20$ l/min. ■, $V_a = 30$ l/min.

Clearly, since the calibration of the UV data is unknown, there is an arbitrary factor in the magnitude of the measured transfer function. In Figure 10, this factor is taken to be the same for the two equivalence ratios. On the basis of the analysis in Appendix A, the best estimate of the function is $|Tr(b/f)| = |\bar{b}^2|/p_f b|$. The measured data with $Co > 0{\cdot}2$ are compared with a function proportional to $\rho c(u_2 A_2 - u_1 A_1)/p_f \equiv (A_2/Z_2) - (A_1/Z_1)$. According to equation (15), this function is proportional to h/p_f and hence to the transfer function, if the coherence is high enough. The areas associated with the velocities are such that the volumetric fluxes are those issuing from the burner, and from the flame into the combustion chamber. Examination of the calculated acoustic impedances shows that, under most circumstances, the function is dominated by the combustion chamber term. The theory is seen to describe the data over considerable portions of the frequency range, although once again, the failure of the measurements to attain the high theoretical values in the ranges < 100 Hz and 400–500 Hz is associated with the loss of coherence in the signals.

The phase of the transfer function is also reasonably well predicted (see Figure 11) apart from in these regions. Note that here all the data are included, irrespective of the coherence. The domination of the combustion chamber term is shown by comparison with the u_2/p_f plot, which is almost identical with the one for the volumetric flux jump. Since acoustic energy must be transmitted up the combustion chamber to match the real impedance of the exit, the predicted phases all lie in the range $\pm 90°$.

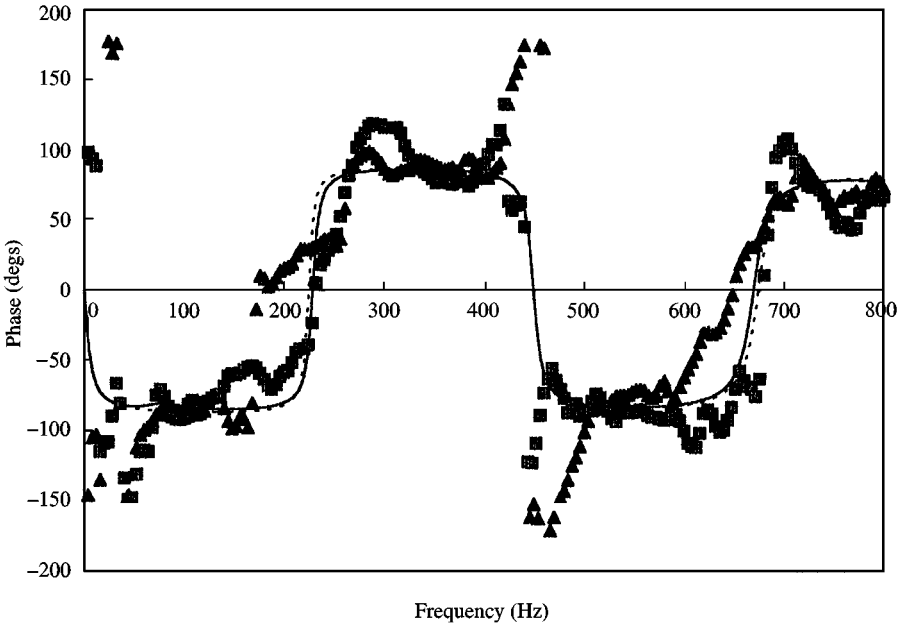

Figure 11. Phase of the total UV emission and the predicted acoustic velocity jump relative to the flame zone pressure for the high impedance plenum (combustion chamber length = 625 mm). ———, theory for $A_2u_2-A_1u_1$, $V_a = 20$ l/min; - - - -, theory for u_2. Total UV emission: ▲, $V_a = 20$ l/min; ■, $V_a = 30$ l/min.

A more interesting presentation from the point of view of analyzing the response of the flame, is that of the phase of the heat release relative to the incident velocity fluctuations u_1 (Figure 12). In some spectral regions where the phase of the inlet impedance is changing rapidly, discrepancies between measurement and theory are put into better perspective by this plot, from which the low coherence data have also been eliminated. Good agreement is now seen across most of the spectrum. The data for the low impedance plenum were qualitatively similar.

Those for the long furnace (and the high impedance plenum) were also similar, with more distinctive peaks now appearing in the magnitude of the transfer function (Figure 13), these corresponding to the half-wave and full-wave frequencies. Discrepancies remained in the data for the phase of the UV emissions relative to the flame zone pressure (Figure 14), but again these are mostly eliminated by the adoption of the $Co > 0{\cdot}2$ criterion in the plot of phase relative to the burner exit velocity (Figure 15). A residual discrepancy around 200 Hz could well be significant, but this plot does show that the small theoretical difference for the two flow rates is mirrored in the measurements.

The most convincing demonstration that the UV emissions are indeed reflecting the thermo-acoustic theory for the flame is provided by replotting the data for a flow rate of 20 l/min and the high impedance plenum feeding different combustion chambers (Figure 16), and the two plena feeding the shorter combustion chamber (Figure 17). Almost identical comparisons were provided by the data for 30 l/min. The data for the two combustion chambers are quite distinct across the whole

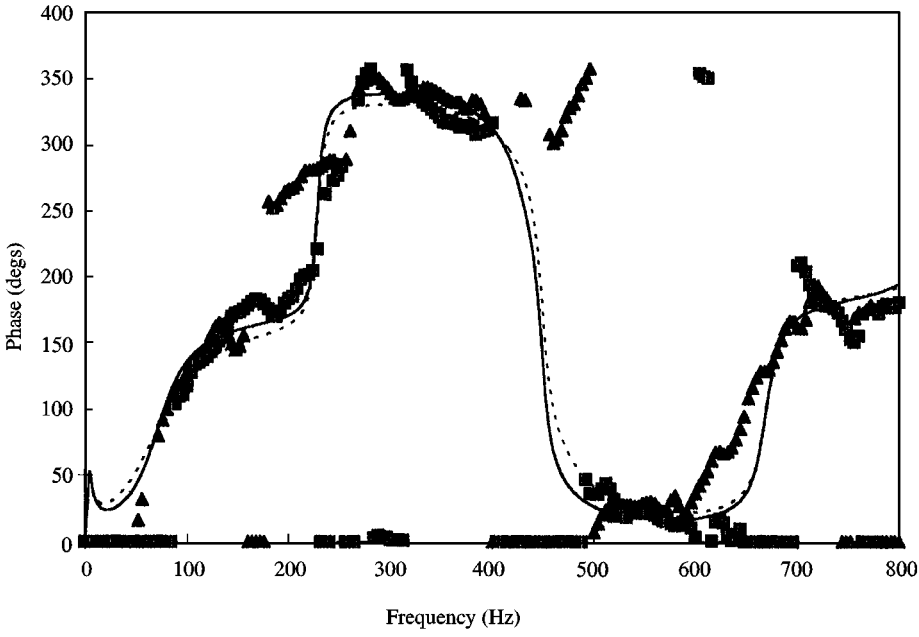

Figure 12. Phase of the total UV emission (with $Co > 0{\cdot}2$) and the predicted acoustic velocity jump relative to the burner exit velocity for the high impedance plenum (combustion chamber length = 625 mm). Theory for $A_2u_2 - A_1u_1$: —— $V_a = 20$ l/min; ----, $V_a = 30$ l/min. Total UV emission: ▲, $V_a = 20$ l/min; ■, $V_a = 30$ l/min.

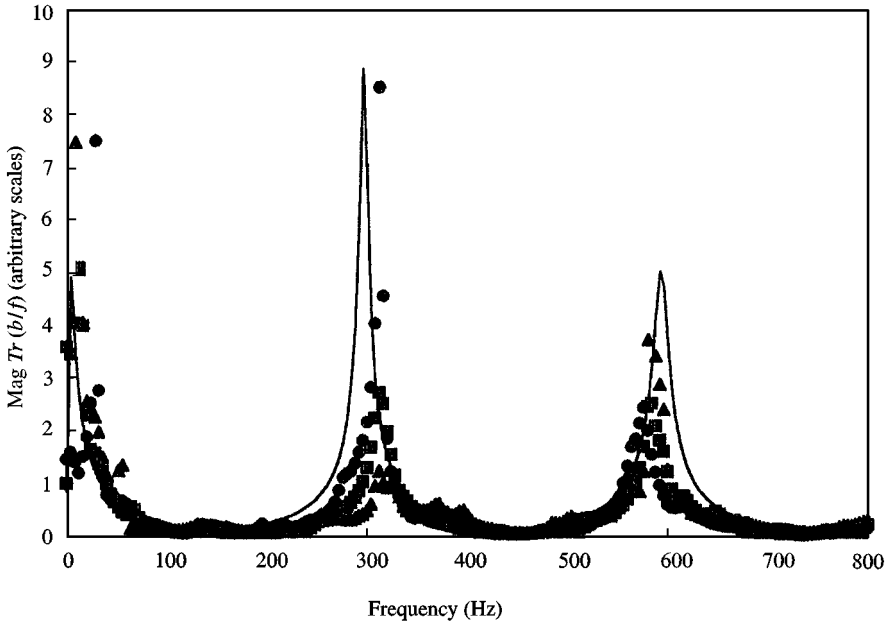

Figure 13. Magnitude of the transfer function between the total UV emission (with $Co > 0{\cdot}2$) or the predicted acoustic velocity jump and the flame zone pressure for the high impedance plenum (combustion chamber length = 888 mm). ———, theory for $A_2u_2 - A_1u_1$, $V_a = 20$ l/min. Total coherent UV emission: ▲, $V_a = 20$ l/min; ■, $V_a = 30$ l/min; ●, $V_a = 24$ l/min.

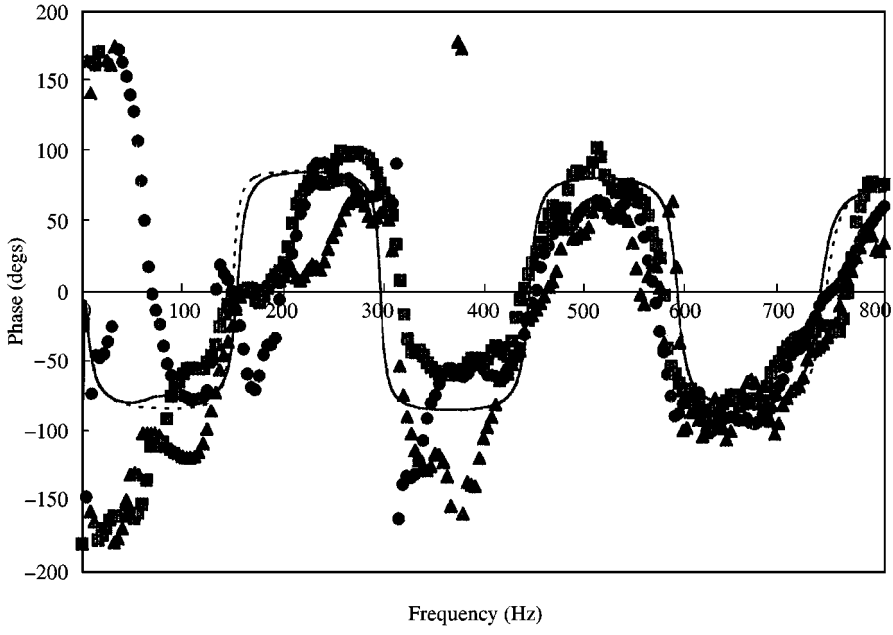

Figure 14. Phase of the transfer function between the total UV emission (with $Co > 0{\cdot}2$) or the predicted acoustic velocity jump and the flame zone pressure for the high impedance plenum (combustion chamber length = 888 mm). ———, theory for $A_2u_2 - A_1u_1$, $V_a = 20$ l/min. Total coherent UV emission: ▲, $V_a = 20$ l/min; ■, $V_a = 30$ l/min; ●, $V_a = 24$ l/min.

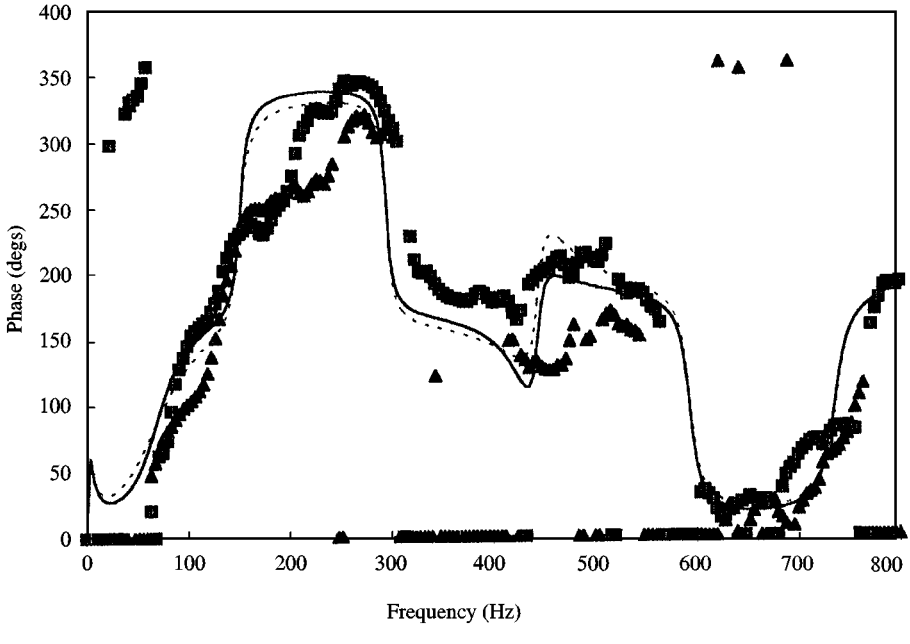

Figure 15. Phase of the total UV emission (with $Co > 0{\cdot}2$) and the predicted acoustic velocity jump relative to the burner exit velocity for the high impedance plenum (combustion chamber length = 888 mm). Theory for $A_2u_2 - A_1u_1$, ———, $V_a = 20$ l/min; - - - -, $V_a = 30$ l/min. Total UV emission: ▲, $V_a = 20$ l/min; ■, $V_a = 30$ l/min.

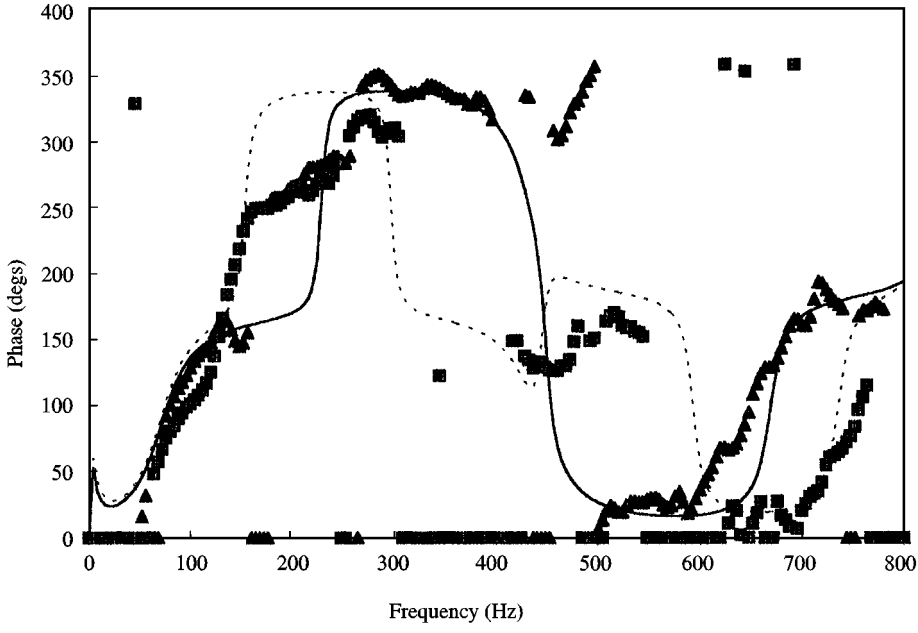

Figure 16. Phase of the total UV emission (with $Co > 0{\cdot}2$) and the predicted acoustic velocity jump relative to the burner exit velocity for the high impedance plenum and two combustion chamber lengths ($V_a = 20$ l/min). Calculated phase of A_2u_2–A_1u_1: ———, $l = 625$ mm; - - - -, calculated phase of $A_2u_2 - A_1u_1$, $l = 888$ mm. Phase of total UV emission: ▲, $l = 625$ mm; ■, $l = 888$ mm.

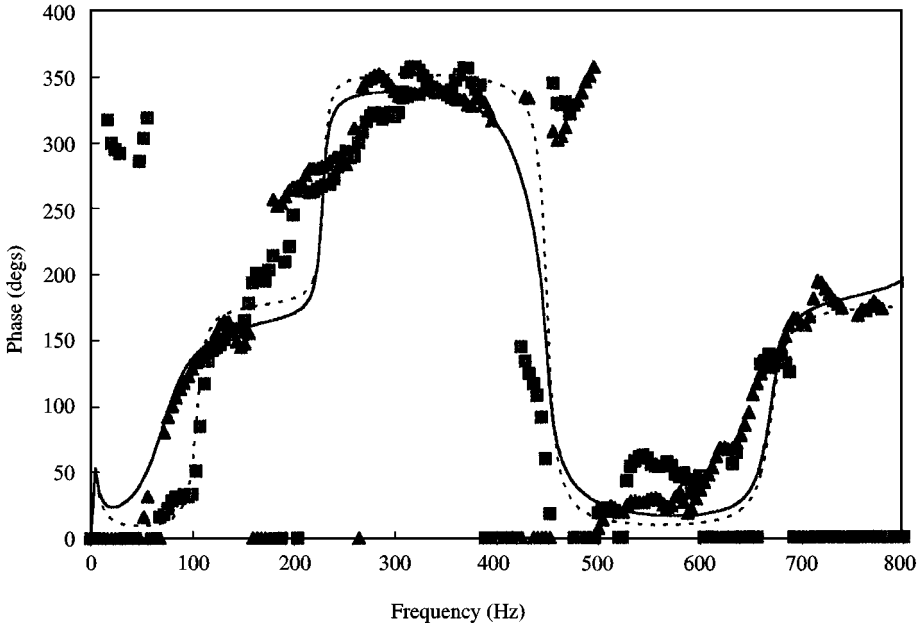

Figure 17. Phase of the total UV emission (with $Co > 0{\cdot}2$) and the predicted acoustic velocity jump relative to the burner exit velocity for the two plena and a combustion chamber length = 625 mm ($V_a = 20$ l/min). Calculated phase of A_2u_2–A_1u_1: ———, high impedance plenum; - - - -, low impedance plenum. Phase of total UV emission: ▲, high impedance plenum; ■, low impedance plenum.

spectrum, while those for the two plena only deviate in the region of the Helmholtz resonances at 75 and 110 Hz.

6. DISCUSSION

The flame in these experiments was small in comparison with the combustion chamber dimensions, but distinct changes of shape were seen when it was excited. Tongues of flame burnt back into the annular flow of premixture around the recirculation zone, the blurred shape of the flame being different according to which mode was predominant.

Under all conditions of operation, there tended to be a short initial period in which discrete audible tones were emitted. After this, there was always excitation across broadbands of the spectrum. Identification of the most strongly excited modes was hindered by this variability in time, which was almost certainly due to the warming up of the glass chamber and the gases within it. Whether the changing impedance due to the changing speed of sound and its distribution up the chamber was the sole factor, or whether the response of the flame also changed significantly, cannot be gleaned from these data. The buoyancy of the gases in the combustion chamber provided a good indication that the average temperature had stabilized before any measurements were taken.

A persistent concern was the validity of the acoustic data when the coherence was low. This condition arises when the magnitude of the components of the pressure fluctuations which are not associated with plane waves is comparable with those that are (see Appendix A). Even in the case of the transfer between two well-separated pressure signals, the correlated components can only be unambiguously identified as acoustic if the decay time of the largest turbulent scales is shorter than the convection time. If this is so, the only errors in the phase measurement should be random ones due to the apparent correlations which can arise from statistically inadequate sampling, but the magnitude of the measured transfer functions can be reduced, as shown in the comparisons with theory, such as those in Figure 4.

With the data confined to cases where the coherence was greater than 0·2, the correspondence of the pressure transfer functions with the 1-D theory is generally satisfactory for both the plenum/burner premixture supply system and the combustion chamber (see Figure 4, 5, 8 and 9). The former confirms that the effect of sudden contractions in flow cross-section and various elements of flow resistance can be described by this means, at least down to wavelengths of the order of seven times the duct diameter.

Nevertheless, the discrepancies in these comparisons require some comment. At those frequencies for which the combustion chamber impedance becomes very small, the acoustic component of pressure fluctuation is so small that it is submerged by the random turbulent fluctuations and the magnitude of the measured transfer function is also too small (400–500 Hz in Figure 4). The discrepancies in the phase ($>$ 700 Hz in Figure 5 and 100–400 Hz in Figure 9) are less easily explained. With account taken of the UV data discussed below, the likelihood is that the acoustic pressure transfer measurements for the combustion

chamber are systematically in error in the range 100–400 Hz, since the theory is adequate in all other respects to describe both the pressure and UV data. Those for the plenum/burner cannot be judged by reference to the UV, since the volumetric flux jump is not sensitive to the u_1 component.

The normalized relationship between the acoustic pressure and UV emission signals, in the form of the magnitude and phase of the transfer function, was not obviously affected by the variability in the excitation, being theoretically constrained by the thermo-acoustic condition [equation (15)] at all frequencies, irrespective of whether they were eigevalues. The analysis in Appendix A recognizes that all of the heat release fluctuations are subject to equation (15), but that not all of the plane wave acoustic velocity fluctuations in the burner generate a spatially coherent response in the flame, since some are due to the integrated effect of random turbulence in the jet and flame, albeit combustion-enhanced. These two contributions can only be rigorously distinguished by forced excitation.

However, the latter would be expected to have a smooth spectral distribution, while the former would be at discrete frequencies. The peaks in the UV spectrum seen in the present work are heavily damped, suggesting that the response of the flame was always in the essentially linear regime, and not limited by the non-linear behaviour which determines the magnitude of high amplitude discrete tones [9]. An approximate calibration of the transducers gives the maximum r.m.s. pressure fluctuation in the combustion chamber as about 100 Pa (at the Helmholtz resonance frequency of the low impedance plenum) and calculations indicate that this was associated with r.m.s. acoustic velocities at the burner exit of 2 m/s, or 40%. No substantial flow reversal, one possible source of non-linearity, should therefore have been involved.

Between 400 and 500 Hz, the use of the transfer function $|\,Tr(b/f)\,| \equiv |\bar{b}^2/\overline{p_f\, b}\,|$, rather than the more conventional $|\,Tr(b/f)\,| \equiv |\,\overline{p_f\, b}/\overline{p_f^2}\,|$, significantly improved the agreement with theory, confirming that it was the noise in the pressure signal that was responsible for the loss of agreement (see Figure 10). In other words, the flame was not able to respond acoustically to the required extent in that frequency band. The criterion $Co(bf) > 0{\cdot}2$ isolated the regions of the spectrum where there was some significant response, and the true eigenvalues of the system could be identified by using more restrictive criteria.

It should be remembered that there are two "adjustable parameters" in the theoretical predictions: the mean speed of sound for the combustion chamber and the absolute magnitude of the transfer function. The different speed of sound for the two chambers is justified by the likelihood of greater cooling in the longer one. The temperatures corresponding to these mean speeds are about 1000 and 800 K. The correction factor for comparing the magnitudes was dependent on the calibrations of the transducers, but a common value was used for all data from the same run.

The major results of this investigation, however, is that the UV emission photodiode, completely independent of the pressure transducers which were used to deduce the volumetric flux jump, does provide data in close correspondence with that jump, if the signal is taken to be proportional to the total heat release fluctuation from the whole flame. Again, some discrepancies are seen in Figures 10, 12, 13 and 15, but Figures 16 and 17 (and the equivalent ones at the higher flow

rate) demonstrate that changes in the length of the combustion chamber and in the impedance of the plenum have the expected effect on the phase of the heat release relative to the acoustic velocity fluctuations at burner exit.

The above data for this flame show that the most strongly excited modes were nearly all determined by the combustion chamber, but that near the Helmholtz resonance frequency of the premixture supply system, the resulting low impedance of the plenum, particularly with the "low impedance" geometry, did have an effect. Large burner velocity fluctuations in response to small fluctuations in the flame zone pressure were amplified by the flame and enhanced the pressure in accordance with the acoustic response of the combustion chamber.

In general, the favoured modes are those corresponding to multiples of a quarter wavelength in the combustion chamber length. The significance of this is that the velocity ratio u_2/u_1 in response to a common p_f is small, so that a given perturbation in p_f generates high u_1. This fluctuation is enhanced by the flame, thus increasing u_2 and p_f. In order for significant energy to be fed into this mode, the heat release and pressure must have a component in-phase, in accordance with Rayleigh's criterion, but since h is almost proportional to u_2, this part of the criterion is satisfied across nearly all of the spectrum. Only when u_2/u_1 is large, is there is a significant gap in the excited frequencies, because there is insufficient energy input from the flame.

To actually quantify the relative energy inputs to the various modes, it is necessary to examine the real component of $p_f h$ or $\mathrm{Re}(p_f b) \equiv \mathrm{Re}(Tr(b/f))\ p_f^2$. When integrated over a frequency band, this has been dubbed the "Rayleigh integral" in reference [10]. The integrand was found to have the greatest positive values at the frequencies where p_f was also large, which is consistent but not conclusive, because the damping is also frequency dependent.

The failure to establish any stable flame at all in the 888 mm combustion chamber with the low impedance plenum was probably due to the proximity of the Helmholtz resonance for this plenum to the quarter-wave mode of the combustion chamber. This is calculated to lead to a band of frequencies from 100 to 150 Hz in which u_2/u_1 is very small. Oscillations, particularly at 110 Hz, probably built up in amplitude to the extent that the flame was extinguished in less than a second Unfortunately, equipment to track the transient from ignition was not available.

The efficacy of using acoustic damping in the burner to suppress such high-amplitude excitation was clearly demonstrated in this study, since in preliminary trials there were also problems of stabilization in the longer furnaces with the larger plenum, but without the gauze resistance in place. However, it is also seen that significant oscillation can occur at the higher frequencies even when there is damping, if the impedance of the combustion chamber is low and the flame has the right characteristics.

The fact that there are substantial differences in excitation in flames with different mean velocities and equivalence ratios, even when the plenum damping is not a factor, shows that the structure of the flame is crucial in determining $\overline{p_f h}$. The excitation of different regions of the flame, and the conditions under which they contribute to a strong response, are being examined. These considerations are the key to the design of practical burners for quiescent operation.

7. CONCLUSIONS

(1) By using the normal turbulent fluctuations, the acoustic characteristics of a combustion system may be determined from acoustic pressure data, even when the flame is not exciting all the frequencies of interest preferentially. (2) One-dimensional theory is adequate to describe the acoustic response of the simple combustion system investigated here. Since many of the relevant elements were present in this system, this result suggests that more complex systems can also be treated in this way. (3) The acoustic theory allows the jump in volumetric flux across the flame to be calculated, and it has been shown that this is indeed proportional to the instantaneous heat release from the whole flame, as recorded by the chemiluminescent UV emission at 307 nm. This is as required by the theory for a "thin" flame. Thus, both the validity of the experimental technique and the applicability of the theoretical assumptions about the flame have been confirmed.

ACKNOWLEDGMENT

Useful discussions with John Fackrell and David Hobson of PowerGen plc, who suggested the outline of the analysis in the Appendix, are gratefully acknowledged.

REFERENCES

1. Lord Rayleigh 1896 *The Theory of Sound*. Macmillan
2. A. A. Putnam 1971 *Combustion Driven Oscillations in Industry*. New York: Elsevier Publishing Co.
3. B. D. Mugridge, 1980 *Journal of Sound and Vibration*, **70**, 437–452. Combustion driven oscillations.
4. G. J. Bloxsidge, A. P. Dowling and P. J. Langhorne, 1988 *Journal of Fluid Mechanics*, **193**, 445–473. Reheat buzz: an acoustically coupled combustion instability.
5. P. Logan, J. W. Lee, L. M. Lee, A. R. Karagozian and O. I. Smith 1991 *Combustion and Flame*. **84**, 93–109. Acoustics of a low-speed dump combustor.
6. A. G. Gaydon 1974 *The Spectroscopy of Flames* London: Chapman & Hall.
7. A. P. Dowling 1995 *Journal of Sound and Vibration* **180**, 557–581. The calculation of thermoacoustic oscillations.
8. L. L. Beranek 1954 *Acoustics*. New York: McGraw-Hill Book Co.
9. A. P. Dowling 1997 *Journal of Fluid Mechanics* **346**, 271–290. Nonlinear self-excited oscillations of a ducted flame.
10. K. R. McManus, U. Vandsburger, and C. T. Bowman, 1990, *Combustion and Flame* **82**, 75–92. Combustor performance enhancement through direct shear layer excitation.

APPENDIX A: THE EFFECT OF COMBUSTION NOISE

Not all of the fluctuations in heat release are due to fluctuations in the velocity through the burner, so high coherence between h and p_f or u_1 is not found across the whole spectrum.

Let

$$h \equiv h_p + h_r = g(\omega)\, u_p + h_r(u_i), \tag{A1}$$

where the first term expresses the response of the heat release to a plane wave incident on the flame, and the second term is the integrated response of all the random variations due to turbulent fluctuations, u_i, within the flame. Similarly, the plane wave velocity fluctuations in the burner can be broken down into

$$u_1 \equiv u_p + u_n\,(u_i), \tag{A2}$$

where u_p is the component which gives rise to a plane wave at the flame, and u_n is due to the integrated effect of random turbulence in the jet and flame, which by definition is not coherent across the flame. Corresponding to u_p and u_n, there are pressure fluctuations in the chamber, p_p and p_n, and also a random component $p_r\,(u_i)$, which is noise due to the turbulent jet, enhanced by the flame, and which has no associated plane wave component in the burner. Thus

$$p_f \equiv p_p + p_n + p_r\,(u_i). \tag{A3}$$

This somewhat artifical breakdown is necessary to allow for the situations where there is no flame but there is measurable noise, or where there is the normal "combustion roar". In the latter case, there are still plane waves in the burner and a component of the pressure fluctuations, p_n, is dependent on the acoustic conditions.

The plane wave components are subject to the acoustic boundary conditions,

$$p_p = Z_1\,\bar{\rho}cu_p \quad \text{and} \quad p_n = Z_1\,\bar{\rho}cu_n \tag{A4}$$

but p_r has no equivalent response. The thermo-acoustic condition discussed in the main text,

$$h \propto u_2 A_2 - u_1 A_1,$$

also applies, so

$$h \propto u_1 \left(\frac{A_2 Z_1}{A_1 Z_2} - 1\right), \tag{A5}$$

and in conjunction with the acoustic boundary conditions, one may write

$$h = R(\omega)u_1 = R(\omega)(u_p + u_n), \tag{A6}$$

where $R(\omega)$ is a purely acoustic response function. The cross-products can now be formally evaluated:

$$\overline{hp_f} = R(\omega)\,(\overline{u_p p_p} + \overline{u_n p_n}) = g(\omega)\,\overline{u_p p_p} + \overline{h_r p_r} \tag{A7}$$

and

$$\overline{hu_1} = R(\omega)(\overline{u_p^2} + \overline{u_n^2}) = g(\omega)\,\overline{u_p^2}. \tag{A8}$$

Equation (A8) shows that $g(\omega)$, the plane wave response function for the flame, is only approximately equal to $R(\omega)$, deduced from the acoustic response characteristics, if this contribution is dominant over the plane wave from the combustion-augmented jet noise. Comparison of equations (A4), (A7) and (A8) shows that $\overline{h_r p_r} = 0$ for this scheme to be consistent. This is feasible, since the heat release and the pressure are related to the turbulent velocities, u_i, through completely different mechanisms.

Equations (A6) and (A7), together with the acoustic boundary condition (A4), show that the coherence function

$$Co \equiv \frac{\overline{(p_f h)^2}}{\overline{p_f^2}\,\overline{h^2}} = \left\{1 + \frac{\overline{p_r^2}}{\overline{p_p^2} + \overline{p_n^2}}\right\}^{-1} \tag{A9}$$

is degraded by the random component in pressure, but that it provides no measure of u_n, which is inseparable from u_p. Moreover, for the transfer function to provide a good estimate of $R(\omega)$, it is necessary to take

$$R(\omega) = Z_1 \bar{\rho} c\, \overline{h^2} / \overline{p_f h}, \tag{A10}$$

rather than

$$R(\omega) = Z_1 \bar{\rho} c\, \overline{p_f h} / \overline{p_f^2}, \tag{A11}$$

because the thermo-acoustic condition applies to all of h, but not to all of p_f.

APPENDIX B

NOTATION

A	cross-sectional area of duct
b	UV emission at 307 nm from whole flame
c	speed of sound
Co	coherence
d	diameter of combustion chamber outlet
$g(\omega)$	response of flame to a plane wave (h_p/u_p)
h	total heat release fluctuations from the flame
k	wavenumber
k^*	complex wavenumber, defined by equation (9)
K	pressure loss coefficient from the plenum to the combustion chamber, referred to the velocity in the burner tube
l	length of duct or combustion chamber
M	Mach number
p	pressure fluctuation
$\bar{P}$	mean pressure
q	heat release fluctuation per unit volume
R	gas constant
$R(\omega)$	acoustic response function ($(\gamma \bar{P}/(\gamma - 1)\,(A_2 Z_1/A_1 Z_2 - 1)$)
t	time
$\bar{T}$	mean temperature
Tr	transfer function
u	fluctuating velocity
$\bar{U}$	mean velocity
V	Volumetric flow rate
x	axial distance
Z	acoustic impedance ($p/\bar{\rho}uc$)
α	parameter in equation (9)
γ	ratio of specific heat capacities
$\bar{\rho}$	mean density
ρ'	density fluctuation
ω	radial frequency

Subscripts

a	of the air
e	of the combustion chamber outlet
f	in the vicinity of the flame
i	inlet; arbitrary component
n	of a plane wave arising from the integrated effect of random flame turbulence
o	outlet
p	of a plane wave incident on the flame
r	random
w	of the premixture supply plenum
1	in the burner outlet
2	in the combustion chamber downstream of the flame